THE ASTROPHYSICAL JOURNAL, 335:803–813, 1988 December 15

A SEARCH FOR NEAR-INFRARED COUNTERPARTS OF *IRAS* EMBEDDED SOURCES IN THE M17 SW GIANT MOLECULAR CLOUD

DEBRA MELOY ELMEGREEN[1]
Vassar College Observatory; and IBM T. J. Watson Research Center

AND

JAMES PHILLIPS, KELLY BECK, HOLLY THOMAS, AND JAMIE HOWARD
Vassar College Observatory

Received 1988 February 1; accepted 1988 June 15

ABSTRACT

Wide-field near-infrared and blue band plates of the region containing the M17 giant molecular cloud complex have been blinked to locate bright near-infrared stars that may be embedded in the M17 SW giant molecular cloud. Twenty such stars coincided with the positions of *IRAS* point sources that appeared embedded based on color-color diagrams. Some of these stars may be the sources of the infrared luminosities. Of the 20 stars, seven were too faint to appear on the *B* band plate. The optical magnitudes and colors determined from the plate image diameters were measured for the other 13 coincident stars; they are most likely upper main-sequence or pre–main-sequence stars with extinctions $A_v \sim 7$ mag. The *IRAS* luminosity-temperature diagram indicates that the embedded sources in M17 are more massive than those in the Orion cloud. Correlations of the source positions with radio and infrared sources are reviewed.

Subject headings: infrared: sources — interstellar: molecules — nebulae: H II regions — nebulae: individual (M17) — stars: pre–main-sequence

I. INTRODUCTION

The M17 nebula is a prominent H II region near the northern end of a giant molecular cloud in the Sagittarius arm, at a distance of 2.3 kpc. The region of the nebula, and the extended molecular cloud known as M17 SW, have been well studied at a variety of wavelengths. Both M17 and the cloud M17 SW are active sites of star formation. Since the M17 SW region is one of the nearest giant molecular clouds in a major spiral arm, it is important to understand its mass and luminosity distribution in order to better understand sites of massive star formation. Near-infrared observations of the H II region revealed an OB association (Sharpless 1953, Chini, Elsässer, and Neckel 1980). Radio continuum (Wilson *et al.* 1979), far-infrared (Gatley *et al.* 1979), and CO (Lada 1976) observations provided a detailed study of the emission region. High angular resolution CO maps of the molecular cloud near M17 revealed a peak which is coincident with far-infrared emission (Thronson and Lada 1983 and references therein). Lemke and Harris (1981) found 10 discrete sources in the vicinity of the nebula by mapping at 2.2 μm, although several of the sources had kinematic distances beyond the M17 region.

Millimeter-wave CO observations of the extended molecular cloud complex revealed three 15–20 K peaks along the 160 pc length (Elmegreen, Lada, and Dickinson 1979, hereafter ELD). Far-infrared (Stier *et al.* 1982) and radio continuum (Jaffe, Stier, and Fazio 1982, hereafter JSF) measurements indicated the presence of B stars throughout the cloud complex; there are 10 far-infrared sources with luminosities of $2 \times 10^4\ L_\odot$ spread over 100 pc, of which six are near CO peaks. Stutzki *et al.* (1988) estimated that 20–50 B stars could account for the observed [C II] line emission. The formation mechanism for massive star formation was also investigated by Jaffe and Fazio (1982; see references therein), who suggested either a stochastic process or spiral density wave trigger for star formation. A sub-mm CO map of the same region was made by Schulz and Krugel (1987). The HNCO (Snell *et al.* 1984) and CS (Snell *et al.* 1984; Mundy *et al.* 1986) emission evidently comes from clumps 0.7 pc in size that are embedded in the dense cores. The gas associated with protostars in the region was observed by Snell *et al.* (1986). Massi, Churchwell, and Felli (1988; see also references therein) made VLA observations of NH_3 and H_2O in the ultracompact H II region M17-UC1 that suggested the presence of 10^7 cm^{-3} clumps of gas in a 300 $M_\odot$ molecular blob, while near the ionization front a B0 star has formed.

The present study compares *B* and *I* band photographic plates of a 25 degree^2 region around the M17 giant cloud complex to search for bright near-infrared stars (BIRS), as discussed in § II. While most are likely to be line-of-sight M stars, some are probably embedded early-type stars or pre–main-sequence stars associated with the molecular cloud. If so, they could provide the luminosity sources for observed *IRAS* point sources. Their distribution and luminosities could be important for initial mass function studies and for future spectroscopic studies of star formation in the region. Thus, the positions of the BIRS were compared with the positions of *IRAS* point sources. Of the *IRAS* point sources that had infrared colors characteristic of embedded sources, 20 were coincident with BIRS. The likelihood that the positional coincidences between the *IRAS* point sources and the BIRS are real is estimated and discussed in § III*a*. *IRAS* point source and optical positions were also compared with previously observed infrared, radio continuum, and CO sources, as discussed in § III.

Seven of the bright near-infrared stars were invisible on the *B* band plate and on the Palomar Observatory Sky Survey print, making them fainter than ~21 mag in the *B* band. The

[1] Visiting Astronomer, Cerro Tololo Inter-American Observatory, National Optical Astronomy Observatories, which are operated by the Association of Universities for Research in Astronomy, Inc. under contract with the National Science Foundation.

magnitudes and $B-I$ colors of the BIRS were determined from the photographic image diameters, using a sequence measured by Chini, Elsässer, and Neckel (1980). These data were used to estimate their spectral types and extinctions, as discussed in § III*b*. Individual sources of interest for further studies are discussed in § III*d*. Results are summarized in § IV.

II. OBSERVATIONS

Photographic plates of the M17 region were observed using the CTIO 0.9 m Curtis-Schmidt telescope. The blue plates were baked IIa-O emulsions with a GG13 filter, giving an effective wavelength of 4360 Å, and the near-infrared plates were silver nitrate–hypersensitized IV-N emulsions with an RG695 filter, giving an effective wavelength of 7780 Å. The plates cover a $5° \times 5°$ area with a scale of $96'' \text{ mm}^{-1}$ and were centered at 18^h12^m, $-16°30'$. An enlargement of the central half of the I band photograph is shown in Figure 1 (Plate 8).

The plates were blinked using a Zeiss comparator, with a 40′ field of view, crosshairs, and an x-y micrometer. The positions of 2031 bright near-infrared stars (hereafter called BIRS) were measured; over 200 of these BIRS are within the 5 K CO contours of M17 SW as measured by ELD. The repeatability of the measurements was 0.25 mm, corresponding to an accuracy of $\sim 25''$. The positions were converted to 1950.0 coordinates through a least-squares fit to the positions of 24 field stars from the SAO catalog. The resultant positions are accurate to $12''.2$ in right ascension and $5''.7$ in declination. These positional accuracies were adequate for comparison with the *IRAS* catalog of infrared point sources, which typically had error boxes of 30″ to 1′.

The *IRAS* point source catalog, obtained on magnetic tape from the Astronomical Data Center at the NASA/Goddard Space Flight Center, contained 1858 *IRAS* sources in the same region around M17. The flux densities of these *IRAS* sources were corrected by 10%–20% according to their color temperatures, following the procedure described in the *IRAS Supplement* (Beichman *et al.* 1985). The ratios of the flux densities are plotted in the color-color diagrams shown in Figure 2. The parallelogram in Figure 2*a* indicates the region of colors occupied by embedded sources outlined by Beichman (1986) for Orion sources and Beichman *et al.* (1986) for sources in dark cloud cores; the rectangle indicates the region occupied by T Tauri stars (Harris 1985; but see the caution by Tereby and Fich 1987). There are 160 *IRAS* point sources in the M17

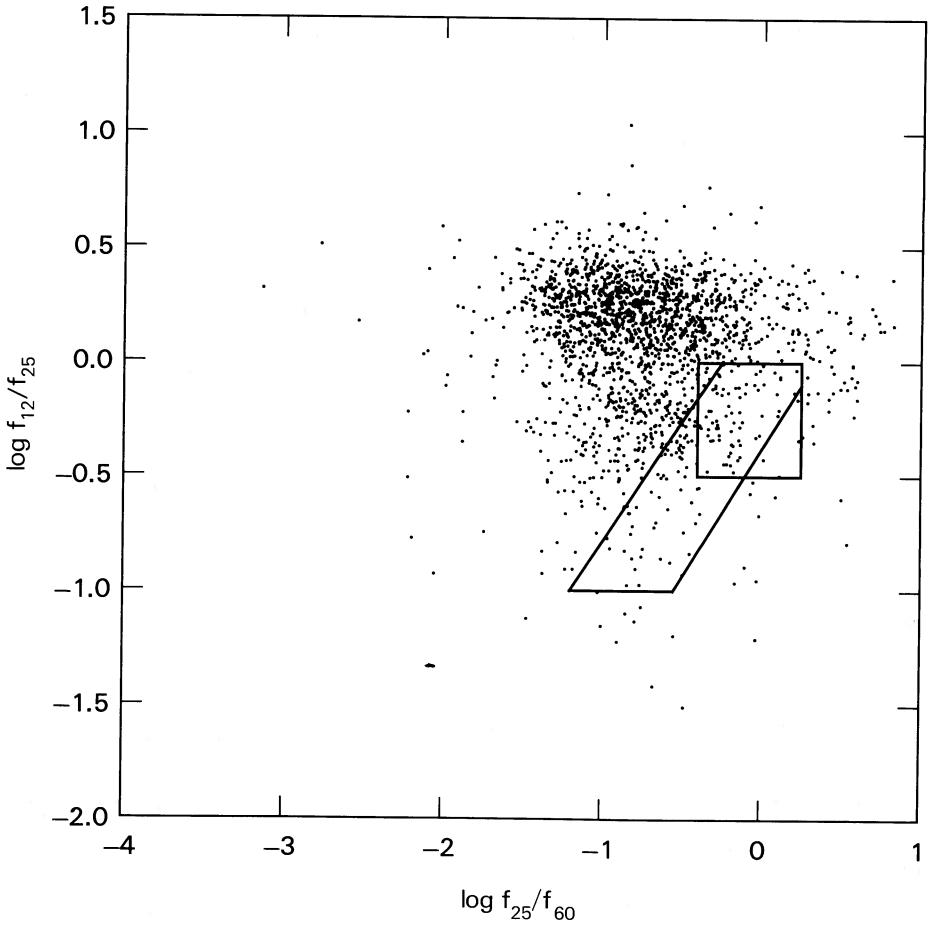

FIG. 2*a*

FIG. 2.—(*a*) All 1858 *IRAS* point sources in the M17 field are shown in this color-color plot, with *IRAS* temperature-corrected flux ratios of 12 μm/25 μm vs. 25 μm/60 μm. The rectangular box indicates the region occupied by known T Tauri stars in other fields (Harris 1985), while the parallelogram indicates the region occupied by sources that probably are embedded, according to the study by Beichman (1986). (*b*) A 25–60–100 μm color-color plot is shown for all of the *IRAS* sources. The small box indicates the region of probable T Tauri stars, while the large box indicates the region of probable embedded stars, according to the table from Emerson (1986).

1988ApJ...335..803E

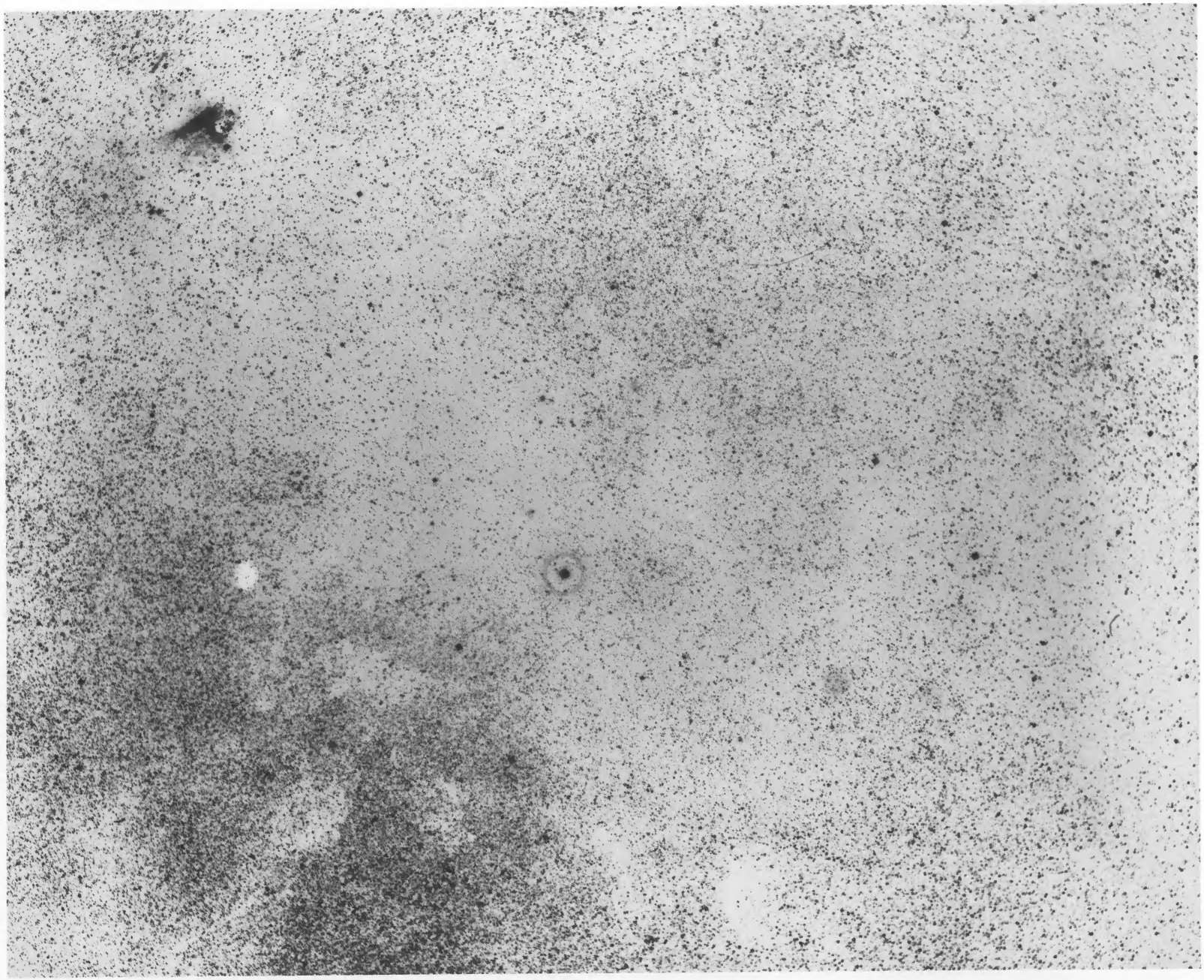

FIG. 1.—The *I* band plate was taken with the CTIO Curtis-Schmidt telescope with a IV-N emulsion and an RG695 filter. This enlargement shows the central half of the plate, with M17 in the upper left, the Saggittarius small star cloud in the lower left, and the molecular cloud complex running diagonally down from M17.

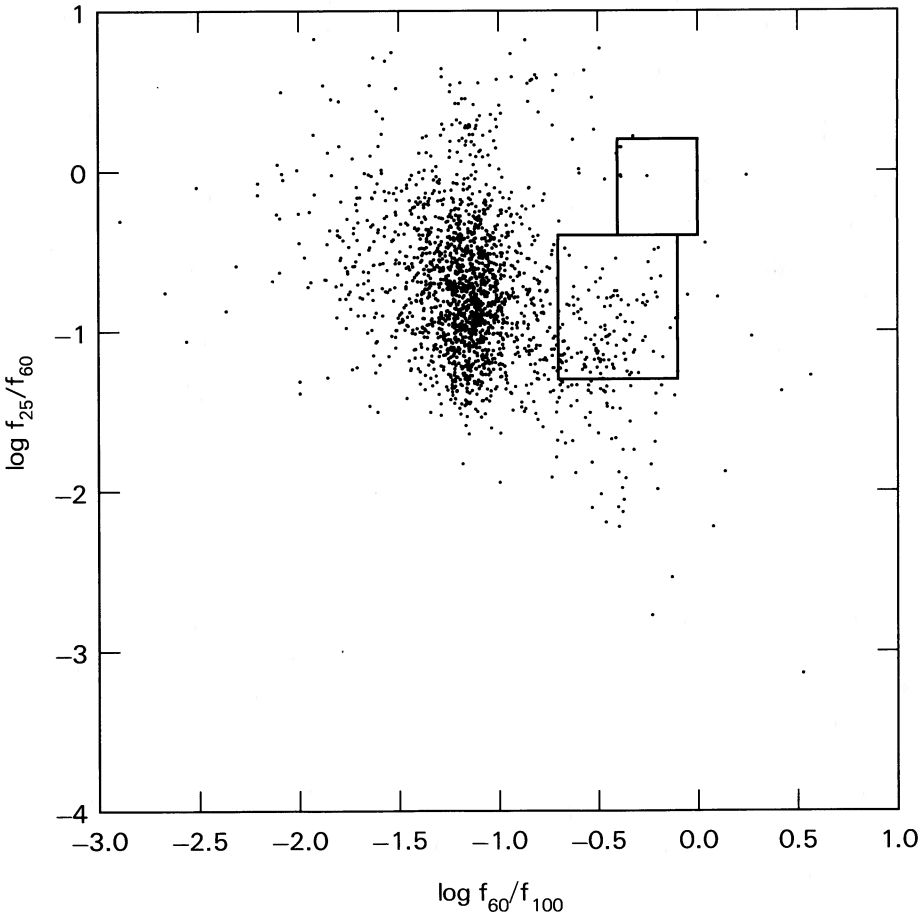

FIG. 2*b*

area in these two boxed regions. The rectangles in Figure 2*b* outline the colors of embedded or T Tauri objects in the 25–60–100 μm diagram, from Emerson (1986); there are 20 *IRAS* point sources in M17 that fall in this region. Nearly all of the 360 *IRAS* objects lying in the 12–25–60 μm or 25–60–100 μm embedded-star ranges are in obscured regions on the Palomar Observatory Sky Survey, and many are associated with far-infrared and radio continuum sources (from JSF). These *IRAS* sources each have emission in all four *IRAS* bands.

Of the 1858 *IRAS* point sources in the M17 region, only 22 satisfy both the 12–25–60 μm and the 25–60–100 μm criteria for embedded stars, as defined by Beichman and Emerson; Table 1 lists these sources. Columns (1) and (2) list the positions, column (3) lists the calculated color temperatures based on the 12 μm and 25 μm flux densities, column (4) lists the luminosities calculated assuming a distance to M17 of 2.3 kpc and integrating over the flux densities, and columns (5)–(8) list the color-corrected flux densities. Column (9) indicates other objects within 1′ of an *IRAS* source (§ III*a*); B stands for BIRS from this study, F for FIR 70 μm sources from JSF, R for radio continuum from JSF, N for the NASA list of 2 μm sources (Gezari, Schmitz, and Mead 1984), H for compact H II region (Chini *et al.* 1986*a*, *b*; distances from Wink, Altenhoff, and Mezger 1982), OH for OH/IR stars (Herman, Burger, and Penninx 1986), and CO for 15 K or hotter temperature contours in ELD. The associated sources are identified in Table 2 and their luminosities and kinematic distances, if known, are given. Note that eight of the 10 sources that have a positional association with an *IRAS* source are beyond the M17 cloud, suggesting that the *IRAS* point sources in these cases are also more distant than the cloud, while two have kinematic distances the same as M17. Since M17 is close to the plane, the region studied is likely to contain many line-of-sight sources; it would be useful to determine kinematic distances to the sources of potential interest listed in the tables in order to establish those associated with M17.

III. RESULTS

a) Positional Associations of BIRS and IRAS Sources

Of the 160 embedded source candidates on the 12–25–60 μm diagram, seven had BIRS identified within 1′ of the *IRAS* point source position and an additional 29 had BIRS identified within 2′. Of the 200 *IRAS* embedded source candidates on the 25–60–100 μm diagram, 14 had BIRS within 1′ and an additional 44 had BIRS within 2′. Of the 22 *IRAS* sources satisfying both the 12–25–60 μm and 25–60–100 μm embedded regions, one had a BIRS within 1′, and six more had a BIRS within 2′. Many of these BIRS could be embedded stars or pre–main-sequence stars, as discussed below. Of course, some may be just random positional coincidences and not physical associations.

To test the statistical significance of the coincidences between *IRAS* point sources and BIRS, fake coordinates were generated by offsetting the *IRAS* coordinates by various angles

TABLE 1

IRAS EMBEDDED SOURCES

Position		T_c	log Luminosity	F12C	F25C	F60C	F100C	
R.A. (1)	Decl. (2)	(K) (3)	($L_\odot$) (4)	(Jy) (5)	(Jy) (6)	(Jy) (7)	(Jy) (8)	Association[a] (9)
$18^h03^m36^s.4$	−19°41′29″	142	3.36	3.55	30.12	93.38	153.22	...
18 04 00.5	−14 57 21	145	2.39	0.37	2.79	10.29	18.15	...
18 06 09.7	−19 07 37	164	3.88	7.49	32.00	220.63	971.70	...
18 07 51.3	−19 28 23	156	3.43	3.68	19.42	90.62	277.83	...
18 08 56.7	−18 37 06	158	4.37	46.39	232.90	1056.33	1614.69	H1
18 09 24.7	−18 40 23	169	3.54	4.01	15.08	109.83	420.75	...
18 09 33.8	−18 13 10	188	3.24	4.87	12.28	49.12	177.36	B1
18 11 10.0	−17 29 36	164	4.60	59.42	255.76	1539.50	3858.49	R1
18 11 41.4	−16 46 19	154	4.84	88.23	498.88	3267.01	5808.70	F1, R2, H2
18 11 42.8	−15 55 38	180	3.30	3.88	11.29	62.81	219.81	...
18 12 54.3	−17 34 25	157	3.25	2.17	11.31	72.28	173.85	...
18 13 24.6	−19 42 25	149	4.18	12.03	78.64	695.68	1469.68	...
18 13 26.9	−16 52 23	153	4.63	30.32	179.01	1650.25	4799.73	F2, R3, N1, H3
18 13 56.7	−18 42 47	139	4.42	19.32	182.25	1259.21	2287.18	F3, R4
18 13 56.9	−18 39 04	139	3.55	3.24	30.40	174.61	282.07	...
18 14 33.7	−15 57 30	161	3.55	5.24	24.06	160.54	300.94	F4
18 15 32.0	−19 13 05	198	2.42	0.92	1.97	5.97	27.55	...
18 15 54.9	−15 50 10	146	3.87	7.25	52.29	335.59	673.19	F5, R5
18 15 59.4	−16 48 55	143	4.35	7.43	59.82	908.05	2681.75	F6, CO
18 16 45.5	−16 58 49	211	2.60	1.59	2.75	9.26	40.55	CO
18 17 29.3	−16 12 48	147	4.79	606.09	4290.93	24082.40	62555.59	F7, N2–N9
18 18 14.3	−15 04 50	198	4.07	90.48	192.08	207.90	500.00	OH1

[a] See Table 2 for identification of associations.

between 10′ and 1°. These fake positions were compared with the BIRS positions, and coincidences to within 0.75 and to within 3′ were recorded. We examined the subset of all *IRAS* sources within the CO temperature contours of ELD that had *IRAS* colors inside or within 0.05 of the log 12/25 μm or log 25/60 μm boundaries of the embedded star region in Figure 2*a*. The 188 *IRAS* sources in this subset included 27 sources that were coincident to within 1′ of a BIRS. The number of *IRAS* sources that had associated BIRS was divided by the area over which the coincidences were tested, and this number was plotted versus the area, as shown in Figure 3. Each line corresponds to a different offset. At zero offset (i.e., the true coordinates; *solid line*) the number/area is larger for smaller areas, and approaches a constant at larger areas, as expected if some of the coincidences are true associations. There is an excess of ~15 *IRAS* sources that have BIRS less than 1′ away for the

TABLE 2

ASSOCIATIONS

Name[a]	log Luminosity ($L_\odot$)	Kinematic Distance (kpc)	Comments
H1	...	5.2	
R1 = 13.19+0.04	5.43	5.8	
F1 = 13.88+0.29, R2 = 13.88+0.27	5.32	4.4	Intermediate luminosity
H2	...	5.4	H II region or compact H II region
F2 = 13.98−0.13, R3 = 13.99−0.13	4.74	3.9	
H3	...	3.8	or compact H II region
F3 = 12.43−1.12, R4 = 12.43−1.11	4.89	4.1	
F4 = 14.92+0.07	3.88	3.0	
F5 = 15.19−0.15, R5 = 15.19−0.16	4.41	4.6	
F6 = 14.23−0.64	4.40	2.3	Early B star cluster
F7 = 15.02−0.67	6.48	2.3	
N1 = AFGL 2101	...	...	
N2 = M17S No. 12	...	...	
N3 = M17S No. 3	...	...	
N4 = M17S No. 4	...	...	
N5 = M17S No. 5	...	...	
N6 = M17S No. 6	...	...	
N7 = M17S No. 7	...	...	
N8 = M17S	...	...	
N9 = M17 No. 1	...	...	
OH 1	...	0.55	OH/IR star
B	...	...	

[a] SOURCES.—F = FIR 70 μm sources from JSF. N = NASA list of 2 μm sources in Gezari, Schmitz, and Mead 1984. OH = OH/IR stars from Herman, Burger, and Penninx 1986. B = BIRS sources listed in Table 3. H = compact H II regions in Chini *et al.* 1986*a*, *b*. R = radio continuum sources from JSF.

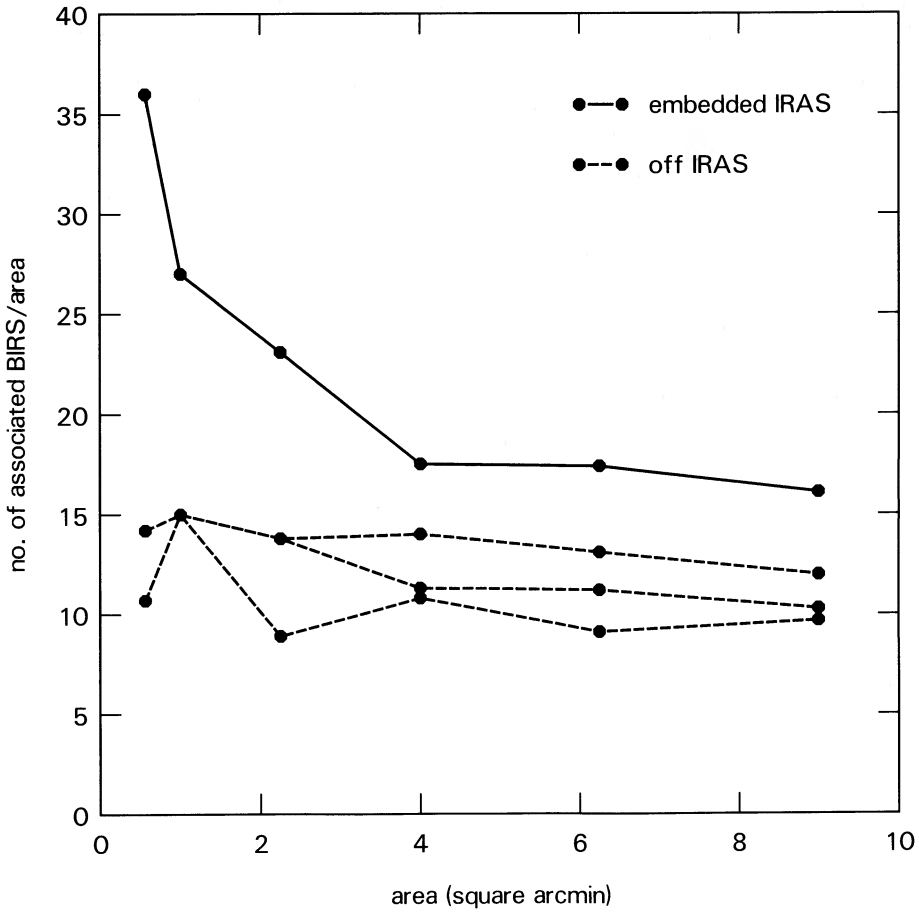

FIG. 3.—The number of BIRS that are less than a coincidence radius away from an embedded *IRAS* source divided by the coincidence area is plotted vs. the area. The solid line represents zero offsets for BIRS and *IRAS* positions. The peak at small coincidence area results from an excess of close coincidences over the random value that occurs at large areas. The dashed lines represent coincidences for BIRS and *IRAS* positions that are offset from each other by three randomly chosen angles greater than 10′. All of the coincidences for the dashed curves should be random. The solid and dashed lines converge at large areas because the random coincidence rate is independent of offset. The figure suggests that approximately 15 BIRS out of the 27 coincidences at 1 arcmin^2 radius are in excess of the randomly expected value, and so are true associations between *IRAS* point sources and near-infrared stellar sources on the *I* band plate.

zero offset coordinates compared with the extrapolated value ($\sim$12) for large offsets. This implies that approximately 15/27 = 57% of the coincidences between *IRAS* sources and BIRS are likely to be true associations. The percentage of agreements is even larger, an excess of 13 out of 20 total stars, or 65%, for a coincidence radius of 0.′75, indicating that several of the *IRAS* positions and BIRS positions match very well.

The coincidence test was also run for all of the 1858 *IRAS* sources and 2031 BIRS. This total sample included 149 coincidences with BIRS less than 1′ away. In contrast to the M17 cloud subset, this sample with zero offset coordinates showed an excess of only 29/149 = 20% that are likely to be true associations. We conclude that the *IRAS* sources in the immediate M17 vicinity that have colors of embedded sources are more likely to be physically associated with coincident BIRS than are random field sources.

The spatial distribution of all of the embedded *IRAS* sources and the BIRS coincident with them is shown in Figure 4. The *IRAS* sources are coded according to how they satisfy the observational criteria for embedded objects. The diagonal concentration of X's in the figure lies along the Galactic plane, and the coincident BIRS roughly outline the region of the giant molecular cloud complex mapped in CO by ELD. These source positions have also been compared with the positions of infrared sources, primarily 2–19 μm (Gezari, Schmitz, and Mead 1984), balloon far-infrared measurements (JSF), and radio continuum measurements (JSF; Wilson *et al.* 1979). There are nine 2 μm sources, seven 70 μm sources, and five radio continuum sources each less than 1′ from an embedded *IRAS* point source in Table 1. All of these associations are within or close to the CO 5 K temperature contour boundaries. There are also eleven 2 μm sources, six 70 μm sources, and two radio continuum sources within 1′ of a BIRS. Their distributions are shown in Figure 5.

b) Magnitudes and Spectral Types of BIRS

The blue and near-infrared image diameters of the BIRS within 1′ of an *IRAS* or other point source were measured using a 10× magnifier, crosshairs, and a *x*-*y* micrometer scale built into the comparator. The diameters were converted to magnitudes using a least-squares fit to the 27 stars in the infrared embedded cluster whose photometric data were obtained by Chini, Elässer, and Neckel (1980). The standard deviation of the magnitude-diameter relationship was 0.7 mag in the *B* band and 0.6 magnitudes in the *I* band for the standard stars, and the reproducibility of the diameter measurement was esti-

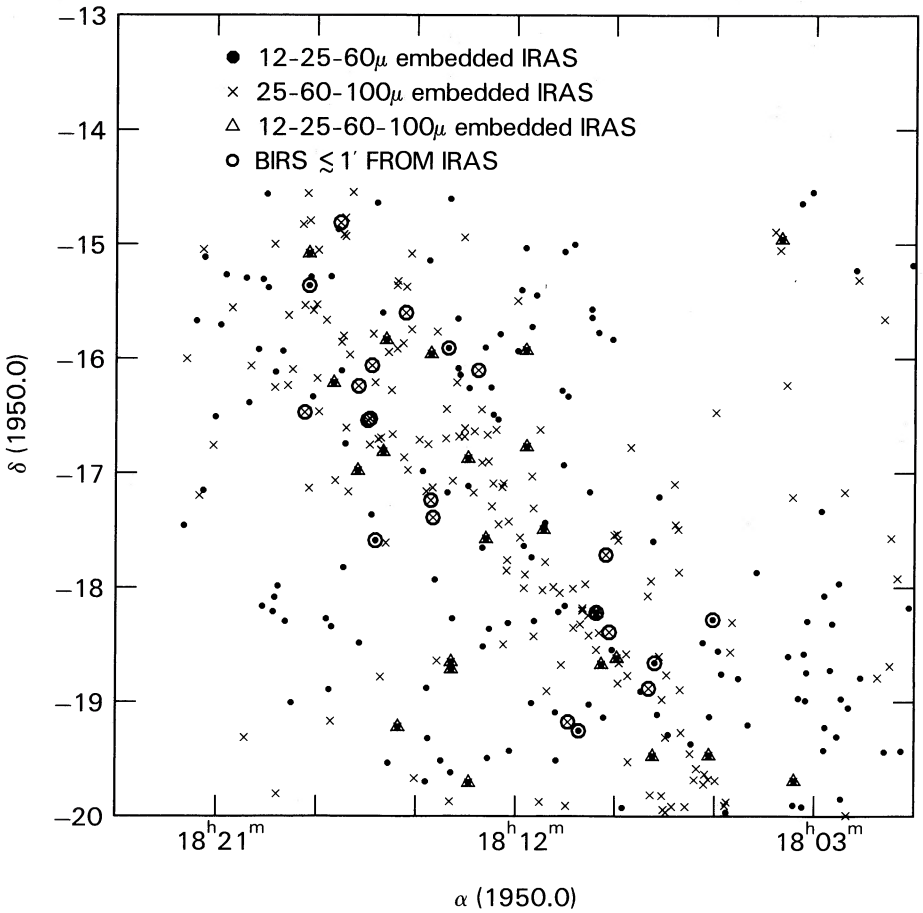

FIG. 4.—The spatial distribution is shown for all of the *IRAS* point sources in the M17 region that have colors typical of embedded sources. Dots satisfy the 12–25–60 μm embedded range, crosses, the 25–60–100 μm range, and triangles, both ranges. Circles represent BIRS less than 1′ from the *IRAS* embedded sources.

mated to be 10%. The BIRS coincident to within 1′ of *IRAS* or other infrared and radio sources are listed in Tables 3A and 3B, respectively.

The apparent magnitudes of the BIRS in Table 3 were compared with the intrinsic I magnitudes and $B-I$ colors of 26 different spectral types listed by Allen (1973), including O5–M5 main-sequence, K0–M5 giant, and K–M supergiant stars. The distances and extinctions of the BIRS that are necessary to reproduce each tabulated spectral type were calculated, and the possible fits (those which required nonnegative extinction values and reasonable distances) were determined for the BIRS. Because our I band had an effective wavelength of 7780 Å, while the listed Johnston I band has an effective wavelength of 7000 Å, the following conversion factor was applied:

$$I_{7780} = I_{\text{Johnson}} + 0.28([V-I]_{\text{Johnson}} - [V-R]_{\text{Johnson}}) \quad (1)$$

for each standard star, following the method of Elmegreen (1980*a*). The I magnitudes and $B-I$ colors of the observed stars then were compared with standard star intrinsic colors in the following way: the color excess given by

$$E(B-I) = (B-I)_{\text{observed}} - (B-I)_{\text{intrinsic}} \quad (2)$$

was calculated for each measured BIRS relative to each spectral type. Assuming a standard reddening law, the I band absorption is given by

$$A_I = 0.48E(B-I) . \quad (3)$$

The necessary distance, r, to match the observed colors of each possible spectral type is given from the distance modulus:

$$\log r = (I_{\text{observed}} - I_{\text{intrinsic}} + 5 - A_I)/5 . \quad (4)$$

There are 20 BIRS less than 1′ away from the embedded *IRAS* sources in Figures 2*a* and 2*b*. Out of the 20 BIRS, seven were visible on only the I band plates and so could not be used to derive spectral types and extinctions; 13 were visible on both the B and I plates. For solutions at a distance of around 2.3 kpc, one set of fits for these 13 stars ranged from types K III to M III with little visual extinction, and another set of fits ranged from types O5 to B5 V with 6–8 mag of extinction. Pre–main-sequence stars occupy similar regions of the color-magnitude diagram, with intermediate extinctions. The possibilities are shown in Figure 6. The solid lines represent the positions of the main-sequence, supergiant, and giant branches. Each dotted line is a range of solutions for a single *IRAS*-embedded BIRS. Each dot corresponds to a solution with a different A_v, ranging from 0.2 mag at the lower right to 10 mag at the upper left, increasing by 0.2 mag per dot. Because these BIRS are associated with *embedded IRAS* sources, they probably have large extinctions, so the main-sequence or pre–main-sequence solutions with high extinctions are preferred. This method is also described in a study of 134 embedded stars in the W3 region by Elmegreen (1980*b*), with similar results. The seven stars that appeared only in the I band could have

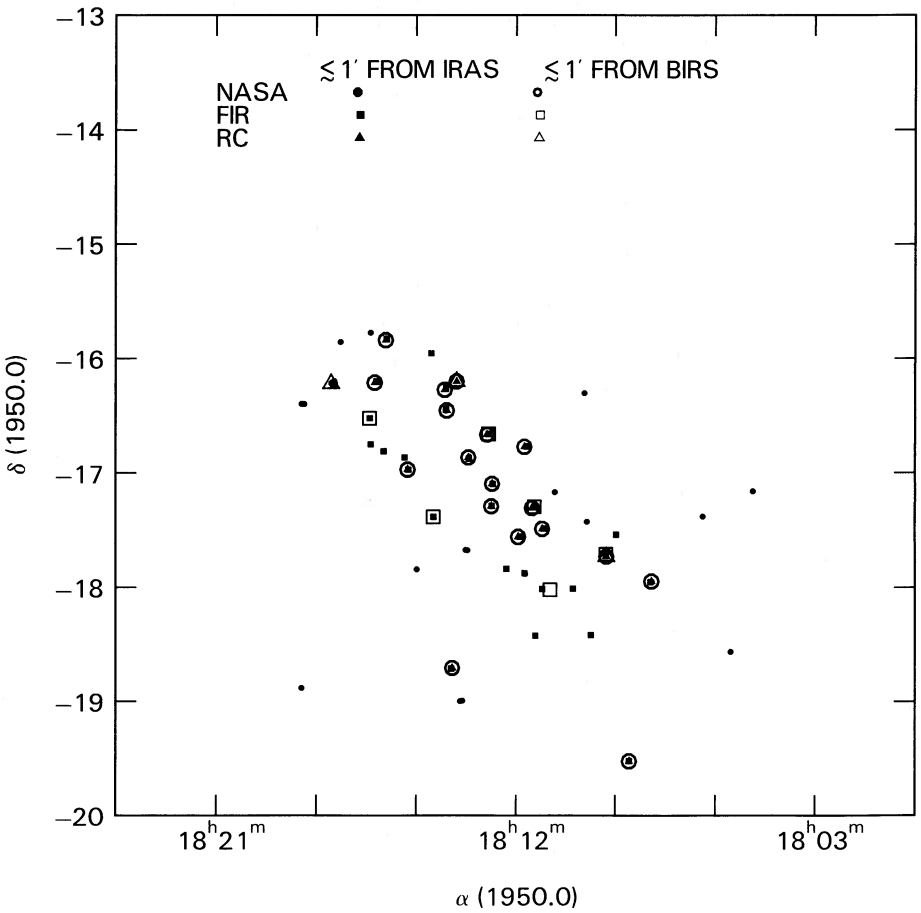

FIG. 5.—The spatial distribution is shown for infrared sources (*circles*) from Gezari *et al.* (1984), and far-infrared (*squares*) and radio continuum sources (*triangles*) measured by Jaffe, Stier, and Fazio (1982), that have coincidences to within 1′ of embedded *IRAS* sources (*open symbols*) or with BIRS (*filled symbols*). These radio and infrared sources were sought only in the immediate vicinity of the M17 molecular cloud, whose boundaries are roughly indicated by the distribution of sources; the largely blank areas were not sampled by JSF.

greater extinctions, lower luminosities, or cooler temperatures than the 13 stars that appeared in both bands. From Table 3, the average *IRAS* luminosity is 6978 $L_\odot \pm 6777$ and 4075 $L_\odot \pm 3628$ for the 13 and seven stars, respectively. These luminosities are consistent with the fainter *B* magnitudes of the seven BIRS relative to the other 13.

To aid in the discrimination of M giants, Dr. Albers of Vassar kindly loaned his IV-N objective prism plates of the M17 region. The approximate magnitude range of the plates included $9 > I > 5$ mag. Two of the 20 BIRS coincident with embedded *IRAS* sources were bright enough (<9th mag) on the objective prism *I* band plates to determine that they are *not* M stars, while three of the BIRS associated with other radio and infrared sources are M giants and one is not.

c) IRAS Luminosities

Luminosities of the *IRAS* embedded sources were determined assuming a distance of 2.3 kpc and a color temperature derived from the 12/25 μm flux densities. Beichman *et al.* (1986) note that the *IRAS* luminosities derived in this way are probably within a factor of 2 of the total luminosities of the sources.

Figure 7 shows a plot of the *IRAS* luminosity versus 12/25 μm color temperature for all 360 objects in the M17 region, with the exception of the sources in Table 1 that are known to be at distances other than 2.3 kpc. The *IRAS* sources with colors matching the embedded regions in all four *IRAS* wavelengths (shown as triangles in the figure) are the coolest, and have color temperatures of about 160 K. The lower bound to the luminosities in the figure is close to the sensitivity limit of *IRAS*, which is about an order of magnitude more sensitive than the balloon survey by JSF. The lowest luminosities detected in M17 by *IRAS* correspond to main-sequence early A stars. Each source has a luminosity that is larger than any luminosities found by Beichman (1986) for 24 embedded sources in Orion that occupy the same positions in the color-color diagrams. Several of the highest luminosity sources studied here have kinematic distances placing them in M17. Evidently, the M17 cloud contains embedded stars of higher mass than the Orion cloud, although both clouds are associated with high-mass nonembedded stars. This may be the result of a different initial mass function for stars in M17 and Orion, or it may indicate a different evolutionary state for star formation in these two regions (e.g., M17 may be younger and less disrupted by massive stars). Gusten and Mezger (1983) and Zinnecker (1987) discussed possible differences in the IMF for clouds located in the main spiral arms and in spurs or interarm regions. Clouds in the main arms, such as the M17 complex, are expected to form more massive stars than are clouds in spurs, such as the Orion cloud.

TABLE 3

BIRS <1′ FROM INFRARED OR RADIO SOURCES

A. BIRS <1′ FROM 12–25–60 μm OR 25–60–100 μm EMBEDDED *IRAS* SOURCES

R.A. (*IRAS*)	Decl. (*IRAS*)	R.A. (BIRS)	Decl. (BIRS)	*B*	*I*	T_c	log $L_\odot$	Comments
18^{h}06^{m}03^s.2	−18°16′40″	18^{h}06^{m}04^s.4	−18°16′35″	>21	11.3	149	4.09	
18 07 48.0	−18 39 30	18 07 44.9	−18 39 13	>21	13.2	210	3.35	
18 07 58.4	−18 52 54	18 07 56.7	−18 52 05	17.1	11.7	140	3.81	
18 09 10.4	−18 23 23	18 09 10.1	−18 23 00	>21	14.7	194	3.77	
18 09 16.9	−17 42 48	18 09 20.1	−17 43 00	15.7	9.4	174	4.27	15 K CO
18 09 33.8	−18 13 10	18 09 37.1	−18 12 56	19.1	12.1	188	3.24	(B1)
18 10 05.5	−19 15 11	18 10 04.2	−19 14 32	17.3	10.5	212	3.44	
18 10 25.3	−19 10 31	18 10 25.9	−19 10 43	18.8	10.6	326	2.70	
18 13 08.8	−16 06 10	18 13 08.4	−16 06 01	19.2	12.0	219	3.82	
18 14 02.8	−15 54 31	18 14 06.2	−15 54 42	15.8	9.4	190	3.45	
18 14 29.8	−17 23 23	18 14 29.8	−17 23 52	13.9	10.9	179	3.99	15 K CO
18 14 33.7	−17 14 15	18 14 33.2	−17 13 56	16.8	9.2	244	3.38	
18 15 19.8	−15 36 03	18 15 19.2	−15 36 36	11.9	8.7	198	3.31	Emission
18 16 13.8	−17 35 19	18 16 13.1	−17 35 08	16.9	10.3	183	2.66	
18 16 20.6	−16 03 42	18 16 17.1	−16 03 28	>21	13.1	222	3.13	15 K CO
18 16 23.9	−16 31 39	18 16 24.3	−16 32 27	15.9	10.8	207	4.30	15 K CO, 2.3 kpc
18 16 27.8	−16 32 28	18 16 24.3	−16 32 27	15.9	10.8	207	4.32	15 K CO
18 16 44.4	−16 14 30	18 16 45.0	−16 13 56	>21	12.5	231	3.41	15 K CO
18 17 18.2	−14 48 42	18 17 16.4	−14 49 11	>21	11.2	246	3.38	
18 18 14.4	−15 21 45	18 18 13.5	−15 21 34	17.1	11.9	236	4.22	
18 18 21.6	−16 28 14	18 18 18.4	−16 27 39	>21	11.7	333	3.25	

B. BIRS <1′ FROM FIR OR RADIO SOURCES

R.A. (BIRS)	Decl. (BIRS)	*B*	*I*	FIR, RC Name	log $L_\odot$	Comments
18^{h}09^{m}16^s.4	−17°43′53″	12.1	8.8	12.76+0.33	...	
18 09 47.3	−17 25 19	11.3	4.0	IRC −20446	...	M spectrum
18 10 47.3	−17 10 34	11.1	4.3	IRC −20450	...	M spectrum
18 10 58.2	−18 0 40	14.5	9.1	12.70−0.17	5.32	3.8 kpc
18 11 28.1	−17 17 13	>21	11.6	13.39+0.08	4.00	2.3 kpc
18 12 49.2	−16 38 54	20.6	14.0	14.10+0.10	3.57	1.6 kpc
18 12 50.5	−16 38 53	18.0	12.9	14.10+0.10	3.57	1.6 kpc
18 13 27.9	−16 41 23	21.6	8.2	AFGL 2103	...	M spectrum
18 13 31.1	−17 40 23	12.2	8.6	AFGL 2102	...	
18 13 32.9	−17 39 42	15.0	8.5	IRC −20455	...	
18 13 33.7	−17 40 0	20.8	11.5	IRC −20455	...	
18 13 33.8	−17 40 29	>21	13.3	IRC −20455	...	
18 13 44.3	−16 11 57	15.3	9.3	14.62+0.12	...	
18 14 16.0	−17 23 10	16.5	13.6	IRC −20456	...	
18 16 24.3	−16 32 27	15.9	10.8	14.63−0.59	4.11	15 K CO, 2.3 kpc
18 17 25.4	−16 11 12	14.2	9.8	M17	...	
18 17 32.0	−16 10 45	13.7	12.3	M17	...	
18 17 33.3	−16 14 27	13.8	9.1	M17A′	...	Not M star
18 17 34.9	−16 13 17	15.2	13.3	15.03−0.69	...	Near Lemke source 3, 2.3 kpc
18 17 38.6	−16 12 14	16.2	10.9	IRC −20466	...	
18 18 18.8	−16 8 52	16.0	12.6	M17D′	...	

d) Individual Sources

The *IRAS* source at 18^{h}09^{m}16^s.8, −17°42′48″ coincides with a 20 K CO temperature contour peak, which has a kinematic distance of 2.3 kpc. It was observed at 70 μm and in the radio continuum at 10.7 GHz by JSF, with an FIR luminosity of $1.9 \times 10^4\ L_\odot$. The luminosity derived from the *IRAS* contributions is the same, 1.86×10^4. The coincident BIRS had $I = 9.4$ mag and $B-I = 6.3$ mag. For an assumed distance of 2.3 kpc, these values correspond to an O5 main-sequence star with 7.8 mag of visual extinction. This optical fit is only about half a spectral class more luminous than the luminosities derived from infrared and *IRAS* observations, so that all observations of the source are consistent with one another.

The embedded *IRAS* sources at 18^{h}16^{m}23^s.9, −16°31′39″ and at 18^{h}16^{m}27^s.8, −16°32′28″ are within a 15 K CO peak and are within 1′ of a BIRS and far-infrared source 14.63−59, which has a kinematic distance of 2.3 kpc. The far-infrared luminosity is $1.29 \times 10^4\ L_\odot$, while the *IRAS* luminosities are $1.99 \times 10^4\ L_\odot$ and $2.01 \times 10^4\ L_\odot$, respectively. The coincident BIRS has a brightness $I = 10.8$ mag and color $B-I = 5.1$ mag; at 2.3 kpc, these values correspond to a main-sequence B0 star with 6.4 mag of visual extinction, which is consistent with the infrared luminosities.

The embedded *IRAS* source at 18^{h}17^{m}29^s.3, −16°12′48″ is in the vicinity of several sources. Lemke and Harris (1981) detected a 2.2 μm source at 18^{h}17^{m}35^s, −16°12′30″ and noted no significant star on the POSS. The radio continuum source at 18^{h}17^{m}32^s, −16°13′05″ detected by Matthews, Harten, and Goss (1979) has a kinematic distance of 2.3 kpc. Lemke and Harris speculate that the 2.2 μm and radio continuum hotspots are not exactly coincident due to variable extinction in the cloud. We find a BIRS at 18^{h}17^{m}34^s.9, −16°13′17″ that is

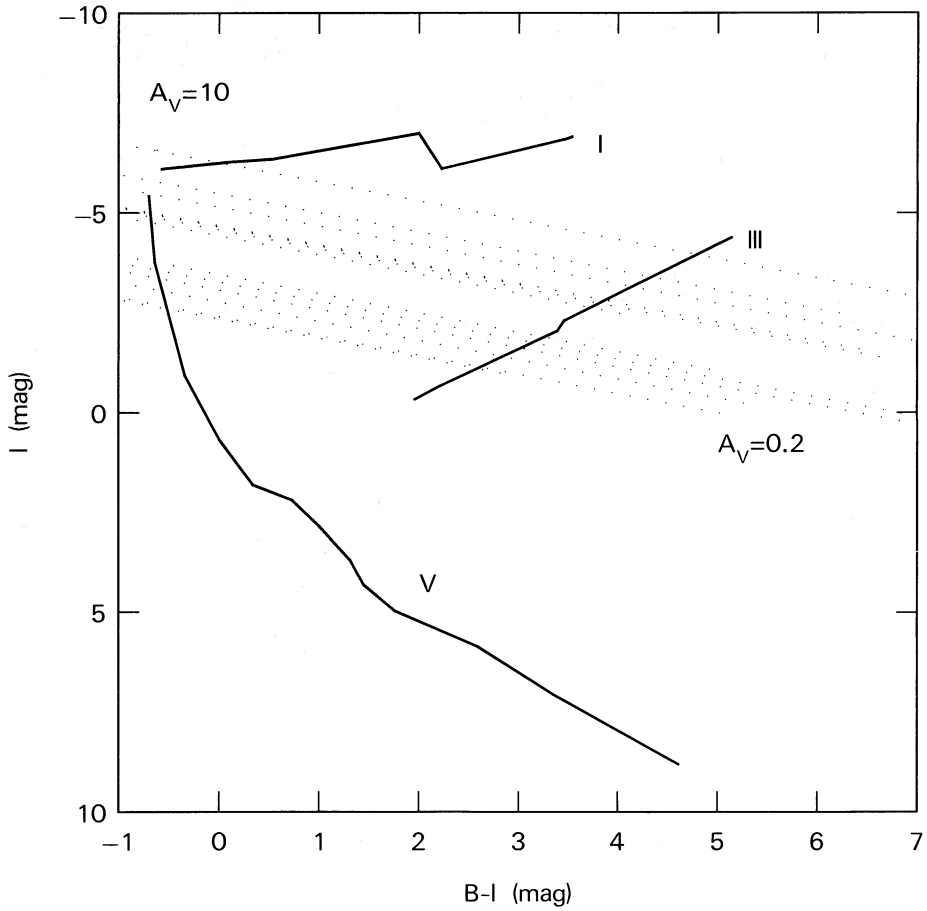

FIG. 6.—This color-magnitude diagram shows as solid lines the I magnitudes and $B-I$ colors of the main-sequence, supergiant, and giant branches. The dotted lines represent the regions of the diagram occupied by the BIRS associated with embedded *IRAS* sources; i.e., the 13 BIRS with measured B and I magnitudes. Their intrinsic magnitudes were derived assuming a distance of 2.3 kpc. The spread of the dots indicates where the stars would lie with different line-of-sight extinctions, ranging from 0.2 mag at the lower right to 10 mag at the upper left, in steps of 0.2 mag of visual extinction per dot. These stars could be supergiant, giant, or upper main-sequence stars, or they could be massive pre–main-sequence stars. Because they are all associated with embedded *IRAS* sources, they are most likely pre–main-sequence or highly obscured upper main-sequence stars.

within 1.5 of the *IRAS* source and within 1′ of these sources. The BIRS, if at 2.3 kpc, has a spectral type of A0 V with 2.1 mag of visual extinction.

A faint, high-extinction BIRS at $18^h11^m28^s.1$, $-17°17'13''$ is near FIR source 13.39+0.08, which also has a kinematic distance of 2.3 kpc.

There are five BIRS in Table 3A that are within 15 K or higher CO temperature contours, and another BIRS that has emission nebulosity associated with it on the blue photographic plate. We plan to obtain high resolution spectra of these BIRS and the other BIRS listed in Table 2 in order to determine their spectral types and luminosities with greater precision.

IV. CONCLUSIONS

In the M17 SW giant molecular cloud complex, there are 360 *IRAS* point sources that are embedded based on 12–25–60 μm or 25–60–100 μm colors; of these, 22 are within the embedded regions on both color-color diagrams. The average 12/25 μm color temperature is 160 K for these 22 embedded sources. Some of these sources correspond to the positions of previously observed compact H II regions, three of which are beyond the M17 cloud. Two embedded *IRAS* sources have positional coincidences with radio continuum sources that are at the 2.3 kpc distance to M17. The luminosities of these 22 sources are greater than the *IRAS* sources in Orion that have the same color ratios. Evidently the M17 cloud contains more massive embedded sources than does Orion, although both have high mass nonembedded stars. This result may be related to the locations of the M17 and Orion molecular clouds in main spiral arm and spur regions of the Galaxy, respectively.

Near-infrared photographic plates are useful for identifying the optical counterparts of *IRAS* sources that are too faint to observe on shorter wavelength photographic plates. We identified 20 bright infrared stars (BIRS) within 1′ of embedded *IRAS* sources. Statistically, we expect that at least 60% of the coincidences are physical associations. Several of the BIRS positions are also within 1′ of other infrared and radio continuum sources. If the BIRS are at the distance of the M17 cloud, then their colors and magnitudes are consistent with B-type stars embedded in ~7 mag of extinction, and their luminosities are consistent with the *IRAS* luminosities. These results support the suggestion by Stutzki *et al.* (1988) that 20–50 B stars may be present in the M17 SW cloud.

Two of the 22 12–25–60 μm embedded *IRAS* sources and five of the BIRS associated with 12–25–60 μm or 25–60–100

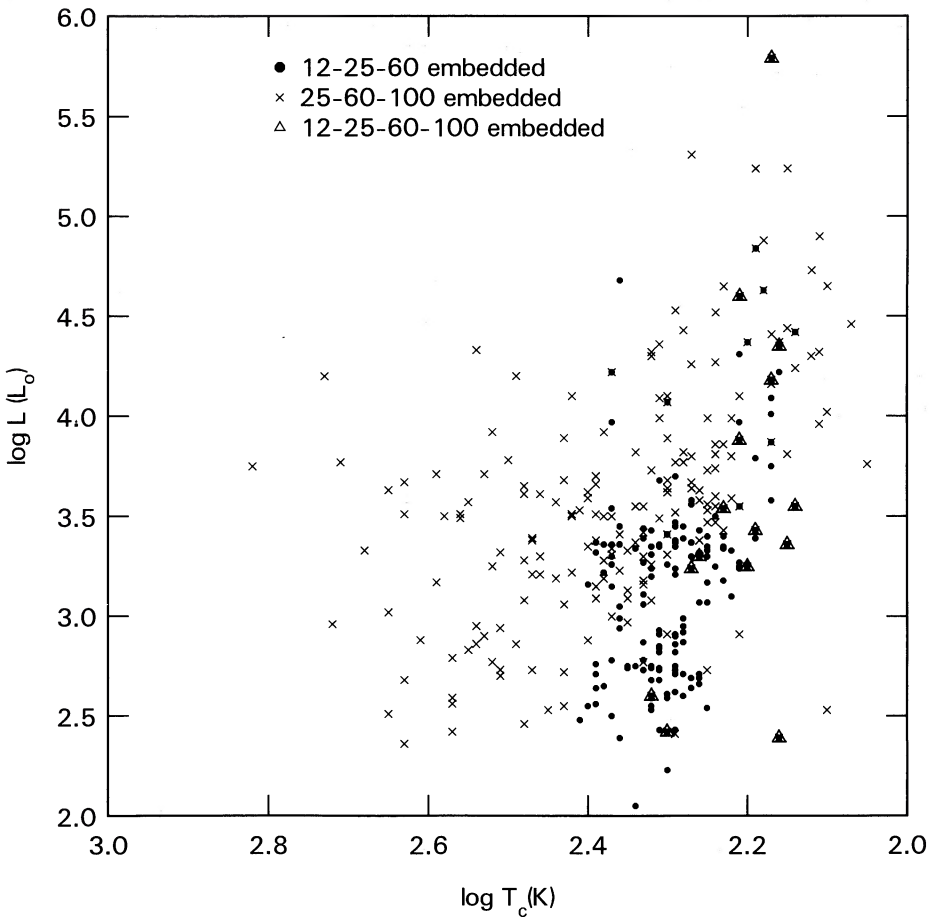

FIG. 7.—A luminosity vs. color temperature plot is shown for all of the embedded *IRAS* sources that appear in Fig. 4, using the same symbols, except that sources listed in Table 1 with distances other than that of M17 have been eliminated. The color temperatures were derived by equating the corrected log 12 μm/25 μm flux density ratio to the corresponding ratio for a Planck function, and the luminosities assume a distance of 2.3 kpc to the sources. This range of luminosities is equivalent to main-sequence stars from late O to late B spectral types.

μm embedded *IRAS* sources are within the 15 K CO contours, and over two dozen *IRAS* embedded sources and BIRS are within 1′ of other infrared and radio continuum sources. More detailed studies of these individual sources may shed further light on the mass distribution within giant molecular clouds.

The authors are grateful to Dr. Fred Chromey for writing a program to extract *IRAS* data from tape, to Dr. Henry Albers for the loan of and assistance with his objective prism plates, and Mr. Jerry Calvin for his reproduction of Figure 1. We benefited from many helpful discussions with Dr. Albers, Dr. Chromey, and Dr. Bruce Elmegreen. D. M. E. thanks the staff at CTIO for observing time, and Dr. Wayne Warren and the Astronomical Data Center at the NASA/Goddard Space Flight Center for providing the *IRAS* data tapes. D. M. E. gratefully acknowledges receipt of a National Science Foundation Visiting Professorship for Women grant. We also thank the Dana Foundation at Vassar College for undergraduate research support.

REFERENCES

Allen, C. W. 1973, *Astrophysical Quantities* (London: Athlone), p. 195.
Beichman, C. A. 1986, in *Light on Dark Matter*, ed. F. P. Israel (Dordrecht: Reidel), p. 279.
Beichman, C. A., Myers, P. C., Emerson, J. P., Harris, S., Mathieu, R., Benson, P. J., and Jennings, R. E. 1986, *Ap. J.*, **307**, 337.
Beichman, C. A., Neugebauer, G., Habing, H. J., Clegg, P. E., and Chester, T. J. 1985, *Explanatory Supplement to the IRAS Catalogs and Atlases* (Washington: GPO).
Chini, R., Elsässer, H., and Neckel, Th. 1980, *Astr. Ap.*, **91**, 186.
Chini, R., Kreya, E., Mezger, P., and Gemund, H. 1986*a*, *Astr. Ap.*, **154**, L8.
———. 1986*b*, *Astr. Ap.*, **157**, L1.
Elmegreen, B. G., Lada, C. J., and Dickinson, D. F. 1979, *Ap. J.*, **230**, 415 (ELD).
Elmegreen, D. M. 1980*a*, *Ap. J. Suppl.*, **43**, 37.
———. 1980*b*, *Ap. J.*, **240**, 864.
Emerson, J. 1986, in *IAU Symposium 115, Star Forming Regions*, ed. M. Peimbert and J. Jugaku (Dordrecht: Reidel), p. 19.
Gatley, I., Becklin, E. E., Sellgren, K., and Werner, M. 1979, *Ap. J.*, **233**, 575.
Gezari, D., Schmitz, M., and Mead, J. 1984, *Catalog of Infrared Observations* (NASA: GPO).
Gusten, R., and Mezger, P. 1983, *Vistas Astr.*, **26**, 159.
Harris, S. 1985, in *Submillimeter Astronomy*, ed. P. Shaver and K. Kjar (Munich: ESO), p. 527.
Herman, J., Burger, J., and Penninx, W. 1986, *Astr. Ap.*, **167**, 247.
Jaffe, D., and Fazio, G. 1982, *Ap. J. (Letters)*, **257**, L77.
Jaffe, D. T., Stier, M. T., and Fazio, G. G. 1982, *Ap. J.*, **252**, 601 (JSF).
Lada, C. J. 1976, *Ap. J. Suppl.*, **32**, 603.
Larson, R. 1986, *M.N.R.A.S.*, **218**, 409.
Lemke, D., and Harris, A. W. 1981, *Astr. Ap.*, **99**, 285.
Massi, M., Churchwell, E., and Felli, M. 1988, *Astr. Ap.*, in press.

Matthews, H., Harten, R., and Goss, W. 1979, *Astr. Ap.*, **72**, 224.
Mundy, L. G., Snell, R. L., Evans, N. J., Goldsmith, P. F., and Bally, J. 1986, *Ap. J.*, **306**, 670.
Schulz, A., and Krugel, E. 1987, *Astr. Ap.*, **171**, 297.
Sharpless, S. 1953, *Ap. J.*, **118**, 362.
Snell, R., Erickson, N., Goldsmith, P., Ulich, B., Lada, C., Martin, R., and Schulz, A. 1986, *Ap. J.*, **304**, 780.
Snell, R. L., Mundy, L. G., Goldsmith, P. F., Evans, N. J., and Erickson, N. R. 1984, *Ap. J.*, **276**, 625.
Stier, M. T., Jaffe, D. T., Fazio, G. G., Roberge, W. G., Thum, C., and Wilson, T. L., 1982, *Ap. J. Suppl.*, **48**, 127.
Stutzki, J., Stacey, J. G., Genzel, R., Harris, A. I., Jaffe, D. T., and Lugten, J. B. 1988, *Ap. J.*, **332**, 379.
Tereby, S., and Fich, M. 1987, preprint.
Thronson, H. A., and Lada, C. J. 1983, *Ap. J.*, **269**, 175.
Wilson, T. L., Fazio, G. G., Jaffe, D., Kleinmann, D., Wright, E. L., and Low, F. J. 1979, *Astr. Ap.*, **76**, 86.
Wink, J., Altenhoff, W., and Mezger, P. 1982, *Astr. Ap.*, **108**, 227.
Zinnecker, H. 1987, in *Evolution of Galaxies*, ed. J. Paloŭs (Prague: Czechoslovakian Academy of Science), p. 77.

K. Beck, D. Elmegreen, J. Howard, J. Phillips, and H. Thomas: Vassar College Observatory, Vassar College, Poughkeepsie, NY 12601